Research Article

Simultaneously Remove and Visually Detect Ce^{4+} Based on Nanocomposite of UiO-66-NH$_2$/CPA-MA

Xiaoqiu Tang,[1,2,3] **Guanghui Wu,**[3] **Tao Wang,**[1,2,3] **Pinghua Chen** [iD],[1,2,3] **Jiezeng Chen,**[1,2,3] **and Hualin Jiang** [iD][1,2,3]

[1]*Key Laboratory of Jiangxi Province for Persistent Pollutants Control and Resources Recycle, Nanchang 330063, China*
[2]*National-Local Joint Engineering Research Center of Heavy Metals Pollutants Control and Resource utilization, China*
[3]*College of Environmental and Chemical Engineering, Nanchang Hangkong University, Nanchang 330063, China*

Correspondence should be addressed to Pinghua Chen; cph1979@126.com and Hualin Jiang; hua20022000@126.com

Effective strategies to deal with rare earth pollution are urgently needed due to the overexploitation of rare earths resource. In this study, a novel nanocomposite of UiO-66-NH$_2$/CPA-MA denoted as UA was successfully synthesized, which can simultaneously remove and detect Ce^{4+} in water. The hybrid consists of UiO-66-NH$_2$ and CPA-MA. Based on the high adsorption performance of UiO-66-NH$_2$, it can remove Ce^{4+} with high capacity by adsorption. Moreover, it can change its color from olive drab to light cyan depending on the adsorbed Ce^{4+} concentration, and the chroma is linearly related to the Ce^{4+} concentration. So, UA can be used to qualitatively and quantitatively detect Ce^{4+} by its color changing. The kinetics of adsorption course was investigated in details. The anti-inference ability of the nanocomposite in coexisting systems was carefully evaluated. The results indicate that UiO-66-NH$_2$/CPA-MA is highly potential to deal with Ce^{4+} pollutions due to its bifunctionality.

1. Introduction

Rare earths are important strategic resources, which are eagerly required in many areas of modern industry. However, overexploitation of rare earth has also brought about serious ecological and environmental problems [1, 2], especially in those countries with vast reserves while relatively low exploitation techniques of rare earth. The effective strategies for dealing with rare earth pollution are urgently needed. Detection and removal are two important aspects for the treatments of pollution [3, 4]. Several techniques have been applied to detect rare earth element (REE) in water, including spectrophotometric method, INAA, MAA, ICP-MS, ICP-AES, and EXAFS. However, most of them require expensive instruments and skilled operators and usually are hard to be used on site. As to the removal of REE in water, sorption is one of the most widely applied techniques because of its cheapness and facile operation [5].

In the previous studies, detection and removal were usually the two independent procedures, resulting toilsome steps and enhancing cost. If these two functions can be incorporated into one material and work simultaneously, the treating efficiency would be highly enhanced.

Metal organic frameworks (MOFs) are a kind of novel materials developing fast in the recent years. They have been widely applied in gas storage and separation, contaminant migration and catalysis [6]. UiO-66-NH$_2$ is a Zr-based MOF which has attracted increasing attention because of its high stability, high adsorption ability, and easy modification. In this study, UiO-66-NH$_2$ was incorporated with chlorophosphonazo-MA (CPA-MA) to construct a novel bifunctional nanocomposite denoted as UA. CPA-MA is a typical spectrophotometric reagent for REE based on its distinctive color changing property as capture REE [7]. The chemical structures of UiO-66-NH$_2$ and CPA-MA are shown in Scheme S1. Based on the high adsorption property of UiO-66-NH$_2$ and the distinctive color changing property of CPA-MA, this hybrid UA can not only effectively adsorb REE but also can significantly change its color when captures the certain REE. The certain color and different

chrominances appearing at different REE concentrations can be used to qualitatively and quantitatively detect the certain REE.

A common REE of Ce^{4+} was used as the model contaminant in this study due to its wide distribution and high hazardousness. UA shows high adsorption capacity toward Ce^{4+}. Furthermore, UA exhibits two different color changing phenomenons in different Ce^{4+} concentration ranges, which could be used to qualitatively and quantitatively detect Ce^{4+} even via naked eyes in rough level, while the precise measurement can be fulfilled by an inexpensive visible-light spectrophotometer. The present study provides a novel effective method to deal with rare earth pollution.

2. Experimental

2.1. Materials. 2-Amino terephthalic acid (NH_2-BDC) was bought from Shanghai Macklin Biotechnology Company, China. Cerium sulfate (Ce (SO_4)$_2$) was obtained from Shanghai Yuanye Biotechnology Company, China. Chlorophosphonazo-mA (CPA-MA) was bought from Sinopharm Chemical Reagent Co., Ltd, China. Zirconium tetrachloride ($ZrCl_4$) was bought from Dongguan Waxi Chemical Company, China. Other chemicals are all commercial. All materials are directly used without further purification with their analytical grade.

2.2. Experiments

2.2.1. Preparation of UiO-66-NH_2. In a typical preparation, 0.2332 g $ZrCl_4$ (1.0 mmol) and 0.1812 g 2-NH_2-benzenedicarboxylate (1.0 mmol) were dissolved in 50 mL N,N-dimethyl formamide (DMF) with magnetic stirring for 30 min to produce uniform dispersion. Then, the mixture was placed into a 100 mL Teflon-lined stainless steel autoclave. It was reacted at 393 K for 48 h. After cooled in air to room temperature, the yellow powder was recovered from the mixture by centrifugation and then washed with DMF and anhydrous ethanol for several rounds. In the end, the powder was dried at 353 K for 12 h to get UiO-66-NH_2.

2.2.2. Synthesis of UiO-66-NH_2/CPA-MA. The hybrid of UiO-66-NH_2/CPA-MA was synthesized by following procedure: 10 mg CPA-MA was dissolved in 40 mL anhydrous ethanol to form a clean solution. 40 mg UiO-66-NH_2 was added and distributed. After that, the suspension was vibrated at 180 rpm for 12 h at 303 K. Finally, the powder was recovered, washed, and dried to get the composite of UiO-66-NH_2/CPA-MA. The synthesized procedure of UiO-66-NH_2/CPA-MA was shown in Scheme S1. The nanocomposite was denoted as UA for the expression convenience.

2.2.3. Characterization. An X-ray powder diffractometer (Cu Ka, Rigaku III/B max) was used to test the samples. Fourier transform infrared (FT-IR) spectra investigation of the samples was conducted on an ALPHA-T FT-IR spectrometer (Bruker, Germany), and the testing range was set as from 4000 to 400 cm^{-1}. The scanning electron microscopy (SEM) imagines of the samples were recorded by a FEI Quanta 200F SEM. The color change of the composite after Ce^{4+}

loading was qualitatively detected by naked eye and quantitatively measured by a solid-state visible spectrophotometer (AvaSpec, China).

2.2.4. Measurement and Removal of Ce^{4+}. Ce^{4+} can be visually detected and simultaneously removed by the UA nanocomposite. 5 mg UA nanocomposite was placed into 10 mL solutions containing different initial concentrations of Ce^{4+} (from 10 to 300 mg/L). The suspensions were vibrated at 180 rpm for 12 h at 298 K. After that, the composite was collected by filtrations. To determine the adsorbed Ce^{4+}, the residue Ce^{4+} concentration was measured by CPA-MA according to the previous report [5, 6], and the adsorbed Ce^{4+} can be calculated by the difference between the original and the residue concentrations. Naked eyes and a solid-state visible spectrophotometer were used to qualitatively and quantitatively investigate the color change of the hybrid after Ce^{4+} loading.

2.2.5. Kinetic Analysis. Kinetic analysis was studied at 298 K with the adsorbent dose of 0.5 g/L. The UA nanocomposite was added into 100 mg/L Ce^{4+} solutions. The mixtures were vibrated at 180 rpm. At different time intervals, the mixtures were sampled to determine the related Ce^{4+} concentration.

2.2.6. Effects of Coexisting Ion Investigation. The coexisting ions effect (Mg^{2+}, Cu^{2+} and Zn^{2+}) toward Ce^{4+} sorption were studied at 298 K. The initial Ce^{4+} concentration was 100 mg/L, while the coexisting ion concentration was set as 0, 100, 150, 200, 250, and 300 mg/L, respectively. The mixtures were vibrated at 180 rpm at 298 K for 12 h. The adsorbent dose is 0.5 g/L.

3. Results and Discussion

The XRD patterns of pristine UiO-66-NH_2 and UA composite are indicated in Figure 1(a). The pristine UiO-66-NH_2 exhibits characteristic peaks at the 7.3°, 8.3°, and 25.6° which are in consistent with the early report, showing the successful synthesis of UiO-66-NH_2 and its high crystallization [8]. These characteristic peaks also appear in the XRD pattern of UA composite, showing the existence of crystal UiO-66-NH_2 in the UA nanocomposite.

FT-IR spectra of UiO-66-NH_2 and UA are indicated in Figure 1(b). As to UiO-66-NH_2, the peaks at 1420 and 1580 cm^{-1} were attributed to C-C vibrational modes and C-O bonding in carboxylates, respectively [9]. 1258 cm^{-1} is ascribed to the C-N stretching of aromatic amines [10]. The adsorption bands at 764 cm^{-1} are ascribed to N–H rocking vibration [9]. The bands located 3475 and 3352 cm^{-1} are designated to the asymmetric and symmetric vibrations of N-H bond in NH_2, respectively [11–13]. These characteristic bands are in consistence with early literatures, confirming the successful synthesis of UiO-66-NH_2. As to CPA-MA, the band located 1676 cm^{-1} is ascribed to the stretching of C=O [14]. It can be found that the typical bands of UiO-66-NH_2 and CPA-MA appear in the spectrum of UA, indicating the well incorporation of UiO-66-NH_2 and CPA-MA, furthermore, peaks related to the NH_2 of UiO-66-NH_2 (3475 and 3352 cm^{-1}) and the peak related to
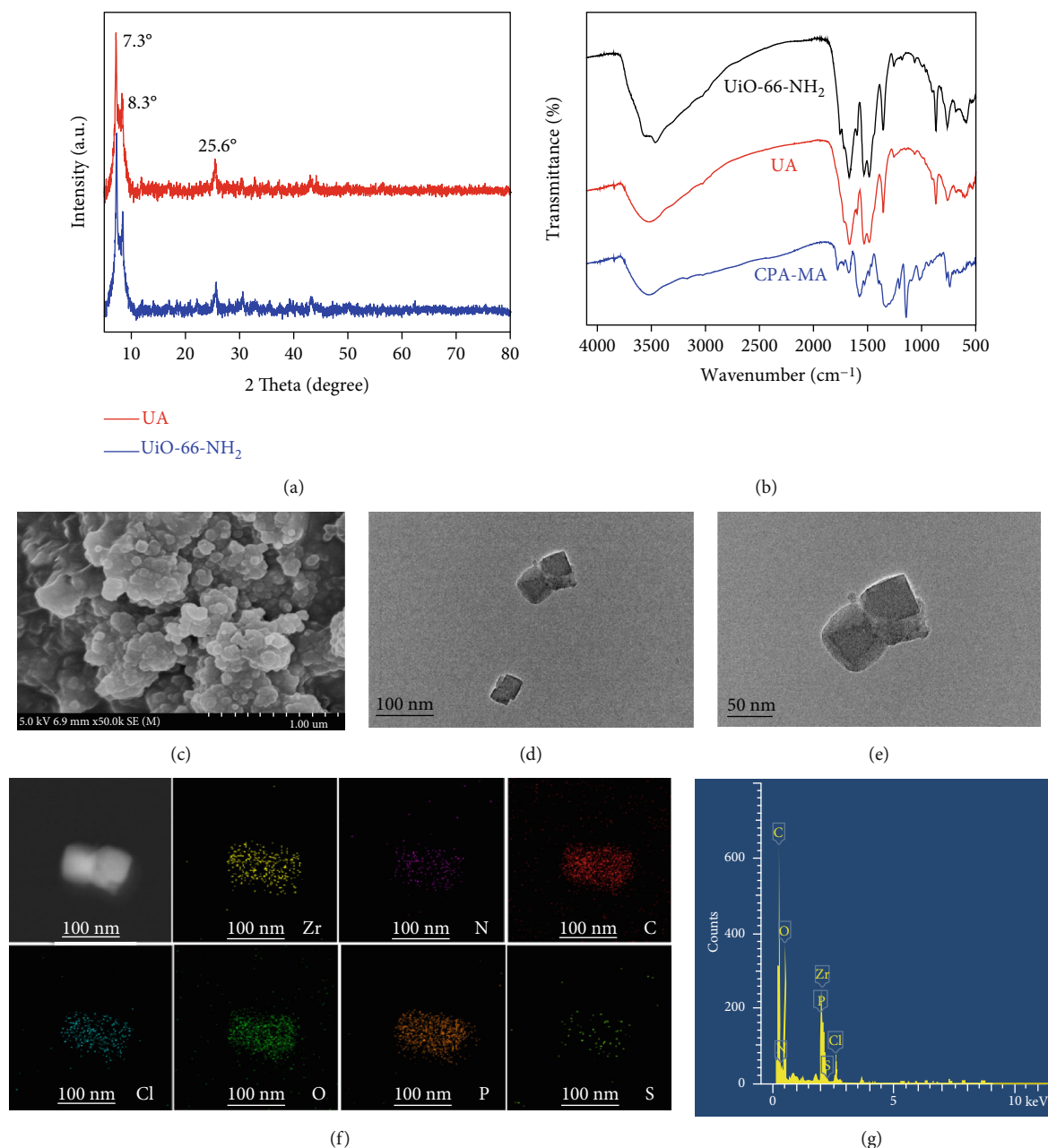
(a)

(b)

(c)

(d)

(e)

(f)

(g)

FIGURE 1: (a) XRD patterns of UiO-66-NH$_2$ and UA composite. (b) FT-IR spectrum of UiO-66-NH$_2$ and UA composite. SEM and TEM images of UA (c)–(e). Elements mapping analysis and EDX pattern of UA (f, g).

the C=O of CPA-MA (1676 cm^{-1}) are all significantly weakened in the spectrum of UA, showing that the NH$_2$ groups in UiO-66-NH$_2$ have condensed with the C=O groups in CPA-MA to form the composite of UA.

As shown in Figures 1(c)–1(e), the SEM and TEM imagines show that the UA nanocomposites exhibits a morphology of cube with the sizes of around 60-80 nm. The chemical composition of UA was further determined by the mapping and EDX analysis (Figures 1(f) and 1(g)). It can be seen that the elements of Zr, N, C, Cl, O, P, and S exist and uniformly distribute in UA composite. These results confirm that UiO-66-NH$_2$ was successfully incorporated with CPA-MA to form the composite of UA.

To investigate the effects of adsorbent dosage toward Ce^{4+} capture, dosage of UA was set from 0.5 to 2 g/L, and the related adsorption capacities are indicated in Figure S1. As one can see that the highest unit adsorption capacity appears when the dosage is 0.5 g/L, so 0.5 g/L was determined as the optimal dosage. The kinetic process of UA adsorbing Ce^{4+} was investigated (Figure S2 (a)). Results showed that the adsorption course was more preferably described by the pseudosecond-order kinetic model (Figure S2 (b), (c) and Table S1). The adsorption capacity of UA was compared with other previously reported Ce^{4+} adsorbents, and the results are shown in Table S2, indicating it being among the top Ce^{4+} adsorbents.
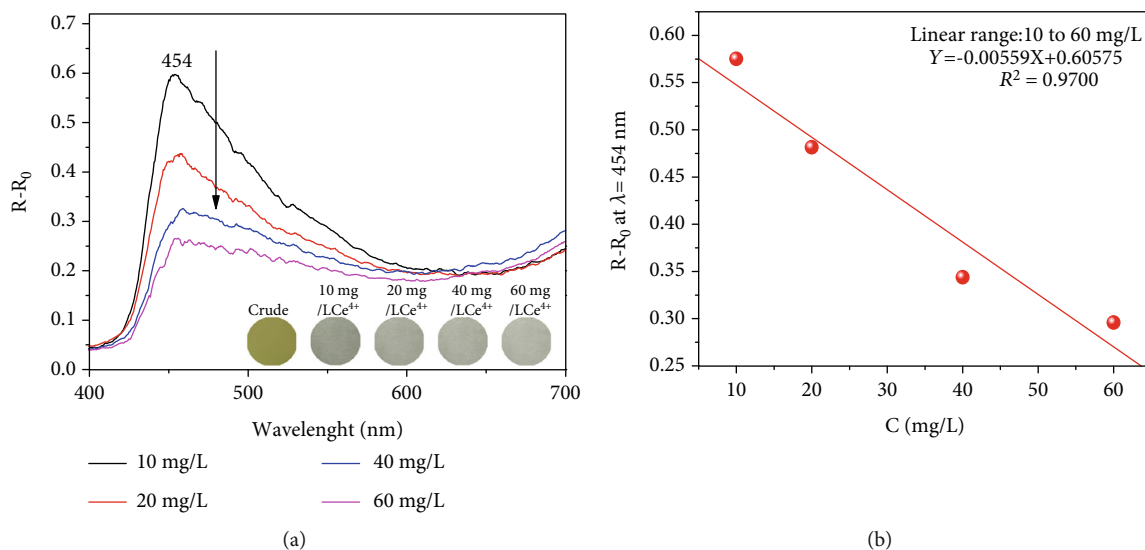
(a)

(b)

FIGURE 2: (a) The UV/Vis diffuse reflection spectroscopy of UA adsorbing Ce^{4+} with different concentrations. (b) The linear relationship spectrum .The experiments were parallel performed in five times. The error bars are shown with absolute values of standard deviation (SD) lower than 3%).
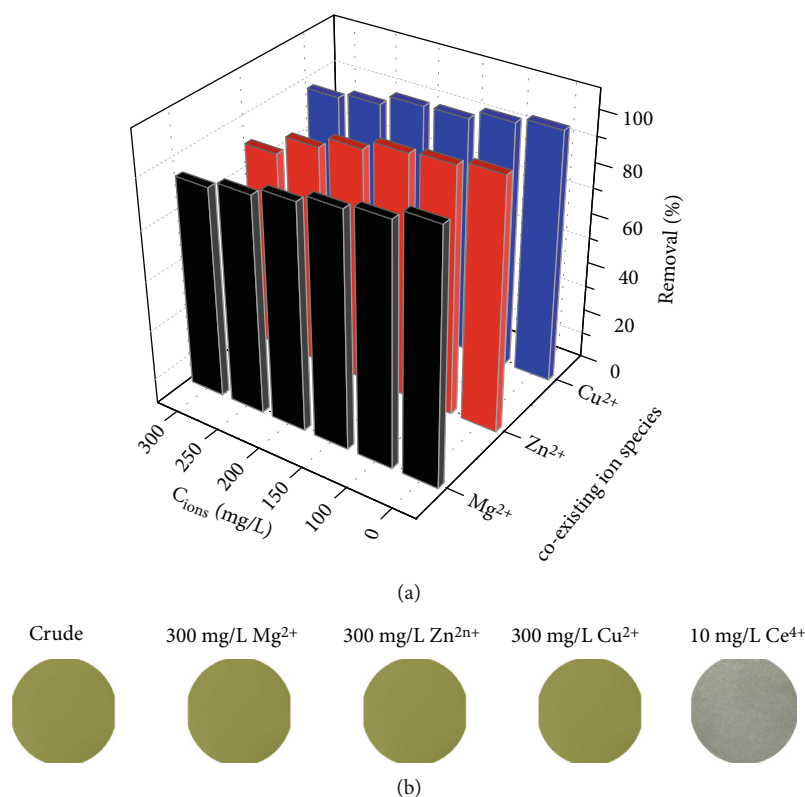

(a)

(b)

FIGURE 3: (a) Effects of coexisting ions on Ce^{4+} adsorption on UA composite (initial Ce^{4+} concentration 100 mg/L, adsorbent dose 0.5 g/L). (b) The color of UA when it captures different metal ions.

In order to test the response of UA toward Ce^{4+}, the adsorptions were conducted with Ce^{4+} concentration, and the related diffuse reflectance spectra reflecting were recorded with a visible light spectrophotometer. The results indicate that the adsorbent can change its color as capturing Ce^{4+} ions with different concentration. The color of crude

UA is olive drab. In the testing Ce^{4+} concentration range, the Ce^{4+} load UA shows light cyan, and the chroma of UA decrease with the increase of Ce^{4+} concentration (insert in Figure 2(a)), which can be testified by the intensity decrease at $\lambda = 454$ nm with the increase of Ce^{4+} concentration (Figure2(a)). Furthermore, as plot the Ce^{4+}

concentration vs. intensity value at 454 nm, it can be found that the intensity changing have linear relationship with the Ce^{4+} concentration, as shown in Figure 2(b). The high coefficience (R^2) values of 0.9700 exhibit the high linear dependence, indicating that Ce^{4+} concentration can be measured by chroma changing of UA.

The limits of detection (LOD) are 3.24 mg/L, which can be calculated by follows:

$$LOD = \frac{3M}{S},\qquad (1)$$

where M refers to the standard deviation obtained in the blank, and S refers to the slope of the linear range in the calibration graph.

So as to study the anti-interference ability, the adsorption capacities of UA toward Ce^{4+} were tested with several coexisting ions (Mg^{2+}, Zn^{2+}, and Cu^{2+}). In the experiments, 100 mg/L Ce^{4+} was paired with 0, 100, 150, 200, 250, or 300 mg/L the competing ion, respectively. It can be seen in Figure 3(a) that the existence of competing ions can affect the adsorption of Ce^{4+} on the nanocomposite in different level, depending on the species. Cu^{2+} shows the least competitiveness, and the nanocomposite removal rate can be retained ~87%. In the presence of Zn^{2+}, which is the most competitive, the nanocomposite removal rate can be retained ~80%. These consequences show that UA has a relatively high anti-interference capacity as adsorbing Ce^{4+}.

The crude UA is olive drab. When UA captures 10 mg/L Ce^{4+}, its color quickly changes to be pale green in seconds. When UA was added to the solution containing other metal ions such as Mg^{2+}, Zn^{2+}, and Cu^{2+}, even their concentrations are 30 times higher than that of Ce^{4+}, and they cannot change UA' color a bit. The results are shown in Figure 3(b), which indicates that Ce^{4+} can be qualitatively detect even by naked eye according to UA's color.

4. Conclusion

In summary, a novel nanocomposite of UA was successfully prepared in this study. It can not only effectively remove Ce^{4+} by adsorption, but can also qualitative and quantitively measure Ce^{4+}. Furthermore, Ce^{4+} ions can be detected by UA with the LOD of 3.24 mg/L. UA has a high anti-interference ability. Several competing metal ions can coexist with Ce^{4+} and will not affect its adsorption and detecting ability. The novel nanocomposite of UA can fast remove hazardous Ce^{4+} ions and can simultaneously visually detect Ce^{4+}. It is a highly potential multifunctional adsorbent to efficiently deal with rare earth containing water.

Data Availability

The data used to support the findings of this study are included within the article.

Disclosure

This manuscript has been post as preprint in https://www.researchsquare.com/article/rs-779280/v1 already [15].

Conflicts of Interest

The authors declare that they have no conflicts of interest.

Supplementary Materials

(1) The effects of adsorbent dosage toward adsorption capacity. (2) The adsorption ability of UA towards Ce^{4+} at different time interval was tested. (3) The pseudo-first-order kinetic and pseudo-second-order kinetic models were used to describe the adsorption course. (4) Comparison of Ce^{4+} adsorption capacity (Q_m) between UA and other previously reported adsorbents. (Supplementary Materials)

References

[1] X. Zheng, D. Wu, T. Su, S. Bao, C. Liao, and Q. Wang, "Magnetic nanocomposite hydrogel prepared by ZnO-initiated photopolymerization for La (III) adsorption," ACS Applied Materials & Interfaces, vol. 6, no. 22, pp. 19840–19849, 2014.

[2] E. Borai, M. Hamed, A. M. el-kamash, T. Siyam, and G. O. el-Sayed, "Template polymerization synthesis of hydrogel and silica composite for sorption of some rare earth elements," Journal of Colloid and Interface Science, vol. 456, pp. 228–240, 2015.

[3] W. Ju, C. Duan, L. Liu et al., "Reduction of cu and nitrate leaching risk associated with EDDS-enhanced phytoextraction process by exogenous inoculation of plant growth promoting rhizobacteria," Chemosphere, vol. 287, article 132288, 2022.

[4] Y. Cui, X. Wang, X. Wang, X. Zhang, and L. Fang, "Evaluation methods of heavy metal pollution in soils based on enzyme activities: a review," Ecology Letters, vol. 3, no. 3, pp. 169–177, 2021.

[5] A. Tanvir, V. P. Ting, and S. J. Eichhorn, "Nanoporous electrospun cellulose acetate butyrate nanofibres for oil sorption," Materials Letters, vol. 261, article 127116, 2020.

[6] L. Shen, M. Luo, Y. Liu, R. Liang, F. Jing, and L. Wu, "Noble-metal-free MoS_2 co-catalyst decorated UiO-66/CdS hybrids for efficient photocatalytic H_2 production," Applied Catalysis. B, Environmental, vol. 166, pp. 445–453, 2015.

[7] Y. Zhu, W. Wang, Y. Zheng, F. Wang, and A. Wang, "Rapid enrichment of rare-earth metals by carboxymethyl cellulose-based open- cellular hydrogel adsorbent from HIPEs template," Carbohydrate Polymers, vol. 140, pp. 51–58, 2016.

[8] Q. Liang, S. Cui, J. Jin et al., "Fabrication of BiOI@UIO-66(NH_2)@g-C_3N_4 ternary Z-scheme heterojunction with enhanced visible-light photocatalytic activity," Applied Surface Science, vol. 456, pp. 899–907, 2018.

[9] K. Y. A. Lin, Y. T. Liu, and S. Y. Chen, "Adsorption of fluoride to UiO-66-NH$_2$ in water: stability, kinetic, isotherm and thermodynamic studies," *Journal of Colloid and Interface Science*, vol. 461, pp. 79–87, 2016.

[10] G. Lv, J. Liu, Z. Xiong, Z. Zhang, and Z. Guan, "Selectivity adsorptive mechanism of different nitrophenols on UIO-66 and UIO-66-NH2in aqueous solution," *Journal of Chemical & Engineering Data*, vol. 61, no. 11, pp. 3868–3876, 2016.

[11] J. Ge, L. Liu, and Y. Shen, "Facile synthesis of amine-functionalized UiO-66 by microwave method and application for methylene blue adsorption," *Journal of Porous Materials*, vol. 24, no. 3, pp. 647–655, 2017.

[12] J. Hou, Y. Luan, J. Tang, A. M. Wensley, M. Yang, and Y. Lu, "Synthesis of UiO-66-NH$_2$ derived heterogeneous copper (II) catalyst and study of its application in the selective aerobic oxidation of alcohols," *Journal of Molecular Catalysis A: Chemical*, vol. 407, pp. 53–59, 2015.

[13] M. Kandiah, S. Usseglio, S. Svelle, U. Olsbye, K. P. Lillerud, and M. Tilset, "Post-synthetic modification of the metal–organic framework compound UiO-66," *Journal of Materials Chemistry*, vol. 20, no. 44, p. 9848, 2010.

[14] Z. Yang, X. Xu, X. Liang et al., "Fabrication of Ce doped UiO-66/graphene nanocomposites with enhanced visible light driven photoactivity for reduction of nitroaromatic compounds," *Applied Surface Science*, vol. 420, pp. 276–285, 2017.

[15] X. Tang, G. Wu, P. Chen, and H. Jiang, "Simultaneously remove and visually detect Ce^{4+} based on nanocomposite of UiO-66-NH$_2$/CPA-MA," https://www.researchsquare.com/article/rs-779280/v1.